Poster presentation | Poster session

Poster Session

Thu. Jul 18, 2024 4:30 PM - 6:30 PM Room P

[PO-06] Numerical Analysis of the Use of Plasma Actuators to Control Pitching and Heaving Motion of an Airfoil

Dereje Arijamo Dolla[1], Yue-Cheng Chung[1], You-Chen Wang [1], *Chin-Cheng Wang[1] (1. National Taipei University of Technology)

Keywords: Flapping wing, Plasma based flow control, Large eddy simulation

[PO-06] Numerical Analysis of the Use of Plasma Actuators to Control Pitching and Heaving Motion of an Airfoil

Dereje Arijamo Dolla, Yue-Cheng Chung, You-Chen Wang, Chin-Cheng Wang*

Computational Physics Research Group
Department of Vehicle engineering, National Taipei University of Technology

July 18, 2024

Contents

CPRG Computational Physics Research Group | National Taipei University of Technology 18 Jul 2024 Page 1

Introduction

- The purpose of this research is to simulatie real-world oscillatory motions such as those seen in flapping wings or vortex-induced vibration.
- Heave-pitch motions affect airfoil performance and stability.
- Heave-pitch motions are critical in applications such as aircraft wings, drones, and wind turbines.
- Dynamic stall, flow separation, and vortex shedding phenomena are challenges in airfoil analysis.

Fig 1. Heave-pitch motion of bird [1]

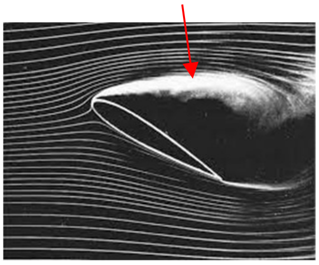

Fig 2. Dynamic stall over an airfoil [2]

- Therefore, this dynamic stall needs to be controlled through plasma actuators to enhance the performance of various aerospace and energy system applications.

[1] Hudson, T., https://en.wikipedia.org/wiki/Bird_flight, retrieved 2024/7/3.
[2] White, F.M., *Fluid Mechanics*, 6th ed., Boston, USA: McGraw-Hill, 2003

Litrature review

- Different studies on airfoil heave-pitch motions (NACA 0012 & 0015) are shown in Table 1 and mainly targeted at improving the power extraction efficiency.

Table 1. Studies on Heave-Pitch Motions at different Reynolds numbers.

Authors	**Method**	**Reynolds number**	**Heave-pitch motions**	**Findings**
Wang et al. [3]	2D CFD	400	NACA 0012 2-DOF passive	FIV dependence on the pivot location and the reduced velocity.
Kinsey et al. [4]	2D CFD	1.1×10^3	NACA 0015 2-DOF active	Heaving amplitude and frequency have the strongest effects on airfoil performances.
He et al. [5]	3D CFD	5×10^5	NACA 0015 2-DOF active	Energy extraction efficiency can reach up to 39%. The effective AoA has a significant effect.
Simpson [6]	Digital PIV	1.38×10^4	NACA 0012 2-DOF active	Energy extraction efficiencies of up to 45%. The highest efficiency regions were all found to exhibit the same 2P vortex shedding.
De Nayer et al. [7]	3D CFD	3.6×10^4	NACA 0012 2-DOF passive	Simulations provide the translatory and rotatory movement allowing to investigate the causes of the observed phenomena.

[3] Z. Wang, L. Du, J. Zhao, M. C. Thompson, and X. Sun, "Flow-induced vibrations of a pitching and plunging airfoil," *Journal of Fluid Mechanics,* vol. 885, A36, 2020.
[4] T. Kinsey and G. Dumas, "Parametric Study of an Oscillating Airfoil in a Power-Extraction Regime," *AIAA Journal,* vol. 46, no. 6, pp. 1318-1330, 2008.
[5] G. He *et al.*, "Modification of effective angle of attack on hydrofoil power extraction," *Ocean Engineering,* vol. 240, 109919, 2021.
[6] B. J. Simpson, "*Experimental Studies of Flapping Foils for Energy Extraction*," Master's thesis, Massachusetts Institute of Technology, 2009.
[7] G. De Nayer, M. Breuer, and J. N. Wood, *International Journal of Heat and Fluid Flow*, vol. 85, 108631, 2020.

Objectives

- Analyze the aerodynamic behavior and flow dynamics of a NACA 0012 airfoil under simultaneous heave and pitch motions.
- Employ large eddy simulation (LES) to capture and understand turbulence effects during the heave and pitch motions of the NACA 0012 airfoil.
- Explore and evaluate the effectiveness of dielectric barrier discharge (DBD) plasma actuators for active flow control in mitigating dynamic stall of the NACA 0012 airfoil.

Governing equations

The contiunity and Navier-Stokes equations for incompressible flow

Continuity equation
$$\frac{\partial \overline{u_i}}{\partial x_i} = 0$$

Momentum equation
$$\frac{\partial \overline{u_i}}{\partial t} + \overline{u_j}\frac{\partial \overline{u_i}}{\partial x_j} = -\frac{1}{\rho}\frac{\rho \overline{p}}{\partial x_i} + \nu \frac{\partial^2 \overline{u_i}}{\partial x_j^2} - \frac{\partial \tau_{ij}}{\partial x_j} + \frac{1}{\rho}F \qquad \tau_{ij} = \overline{u_i u_j} - \overline{u_i}\,\overline{u_j}$$

where, $\overline{u_i}$, $\overline{p}$ are filtered velocity and pressure, ν is the kinematic viscosity, F is body force and τ_{ij} is the subgrid-scale stress tensor

$$F = (f_x)\hat{i} + (f_y)\hat{j} + (f_z)\hat{k}$$

$$f_x = F_{x0}\phi_0^4 \exp\left[-\left(\frac{(-x-x_0)-(y-y_0)}{y}\right)^2 - \beta_x (y-y_0)^2\right]$$

$$f_y = F_{y0}\phi_0^4 \exp\left[-\left(\frac{(-x-x_0)}{y}\right)^2 - \beta_y (y-y0)^2\right]$$

$$f_z = F_{z0}\phi_0^4 \exp\left[-\left(\frac{(-x-x_0)-(y-y_0)}{y}\right)^2 - \beta_z (y-y_0)^2\right]$$

where, F_{x0} and F_{y0} are electrodynamic force, β_x and β_y are functions of the dielectric material. x_0 is midpoint between reference and grounded electrode [8].

$$y = 5ct\left[0.2969\sqrt{\frac{x}{c}} - 0.1260\left(\frac{x}{c}\right) - 0.3516\left(\frac{x}{c}\right)^2 + 0.2843\left(\frac{x}{c}\right)^3 - 0.1015\left(\frac{x}{c}\right)^4\right]$$

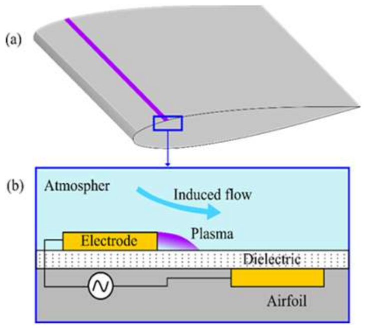

Fig 3. (a) AC-plasma actuator on a NACA 0012
(b) plasma body force formulation

[8] S. Mukherjee and S. Roy, 50th AIAA Aerospace Sciences Meeting, AIAA 2012-0702, Nashville, TN, USA, January 12, 2012.

Computational tool

OpenFOAM and it's structure

- OpenFOAM is a versatile open source CFD toolbox for simulating fluid dynamics and complex physical processes. It's basic structure is shown in figures 4 and 5.
- The pimpleDyMFoam solver is used to simulate the heave and pitch motions of the NACA 0012 airfoil.
- MPI parallelization is employed for efficient computation, reducing simulation time and enhancing scalability.

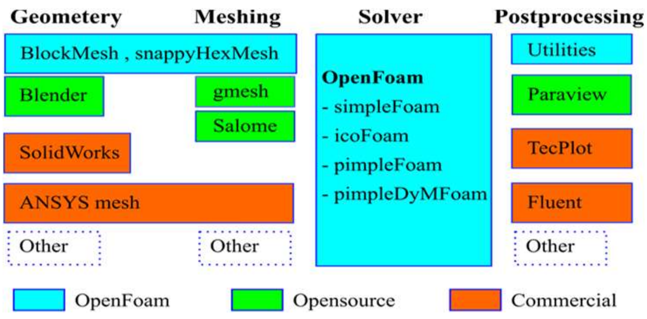

Figure 4. Basic structure of openFoam

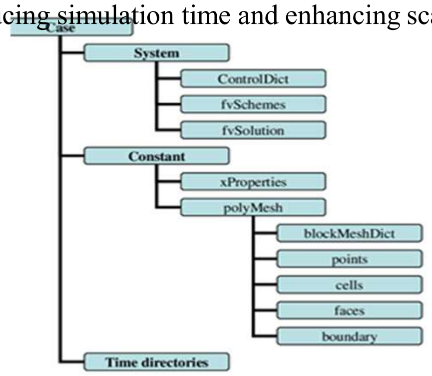

Figure 5. Basic structure of openFoam cases

Problem description

NACA 0012 airfoil with 2-DOF heave-pitch motions in a constant speed is presented in figure 6.

Numerical parameters

- Turbulence model: LES
- Reynolds number: 135,000
- OpenFOAM solver: PimpleDyMFoam
- Freestream velocity: U = 11.53 m/s
- Number of cells: 1.88 million cells
- Center of rotation: 0.25C
- Heave amplitude: 1C (0.15m)

Goal: Analyze the flow behaviour in the heave-pitch motion of NACA 0012 and to control the dynamic stall.

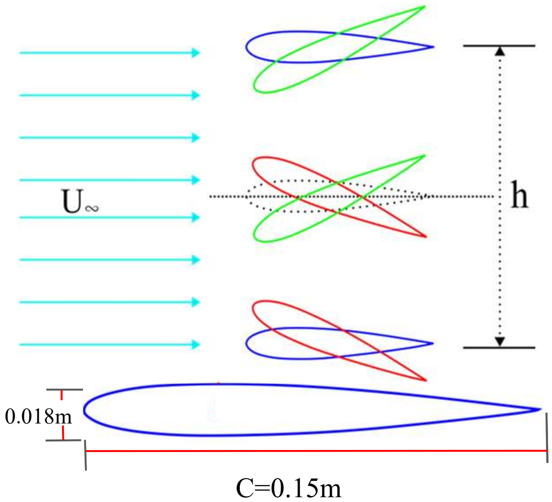

Figure 6. Airfoil in combined heave-pitch motions.

CPRG Computational Physics Research Group | National Taipei University of Technology 18 Jul 2024 Page 4

2-DOF heaving and pitching motions

This elastically mounted airfoil is considered as a linear mass–spring system, and its heaving and pitching motions are governed by the second-order damped oscillator equations [7].

Heaving $$m\ddot{h}+c_h\dot{h}+k_h h-mb\cos\theta\,\ddot{\theta}+mb\sin\theta\,\dot{\theta}^2=F_h$$

Pitching $$I_\theta\ddot{\theta}+c_\theta\dot{\theta}+k_\theta\theta-mb\cos\theta\,\ddot{h}=M_\theta$$

Lift coefficient $$C_h=\frac{F_h}{0.5\rho u^2 A}$$

Moment coefficient $$C_m=\frac{M_\theta}{0.5\rho u^2 cA}$$

Drag coefficient $$C_d=\frac{F_d}{0.5\rho u^2 A}$$

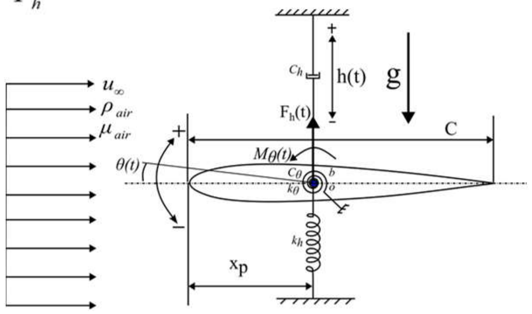

Figure 7. Schematic of 2-DOF heaving and pitching motions [7].

where m and I_θ denote the mass and moment of inertia, b is distance between the pivot location and centre of mass (o), damping factors of c_h and c_θ are zero, F_h and M_θ are lift force and moment.

[7] G. De Nayer, M. Breuer, and J. N. Wood, *International Journal of Heat and Fluid Flow,* vol. 85, 108631, 2020.

Computational domain

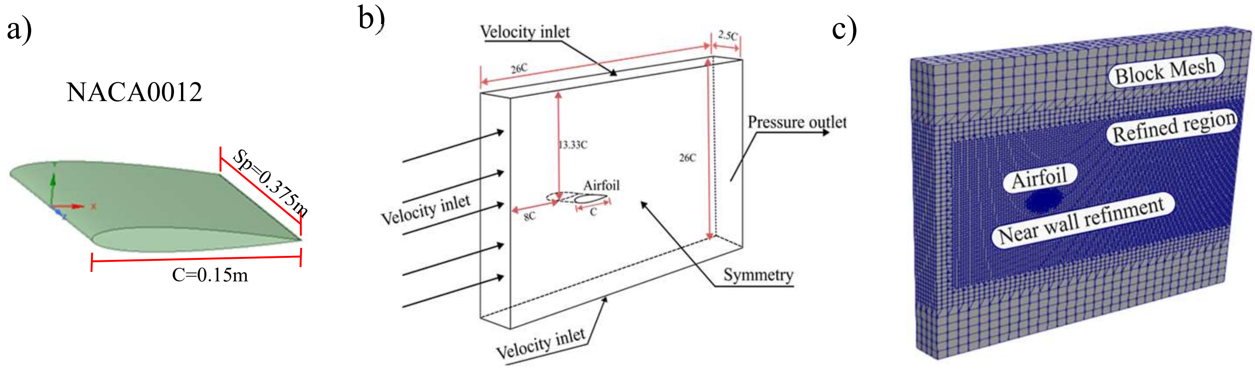

Figure 8. Dimensional parameters (a) Geometry (b) Fluid domain and (c) boundary conditions.

Table 4. Computational doamin test.

Name	Domain	Cl_{rms}	Cd_{avg}	Cl_{rms}/Cd_{avg}
Domain 1	20C × 20C × 2.5C	1.72	1.66	1.03
Domain 2	26.67C × 26.67C × 2.5C	1.71	1.57	1.09
Domain 3	40C × 40C × 2.5C	1.70	1.57	1.08

Verification and validation

Table 5. Static NACA 0012 airfoil grid independence test at different angles of attack compared to Khalid et al. [9].

Name	Total grids	Cl	Cd	Error in Cl (%)
Grid 1	740,051	0.8804	0.4411	1.93%
Grid 2	961,848	0.8712	0.4357	0.87%
Grid 3	1,882,791	0.8621	0.4308	0.18%
Grid 4	3,367,659	0.8623	0.4217	0.16%
Khalid and Akhtar [9]		0.8637	0.4186	

Grid 3 was chosen for its balanced accuracy and computational efficiency.

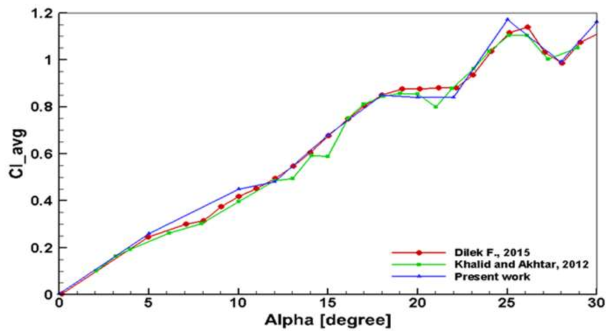

Figure 9. Cl of static NACA0012 airfoil versus AOA with Re=1000.

[9] M. S. U. Khalid and I. Akhtar, 2012 Proceedings of IMECE2012, IMECE2012-87389, Houston, TX, USANovember 9-12, 2012.

Experimental validation

The trend of the present work shown in figure 10 is consistent with Simpson's experimental data, indicating that this computational model of the NACA 0012 heave-pitch motions is suitable as a benchmark.

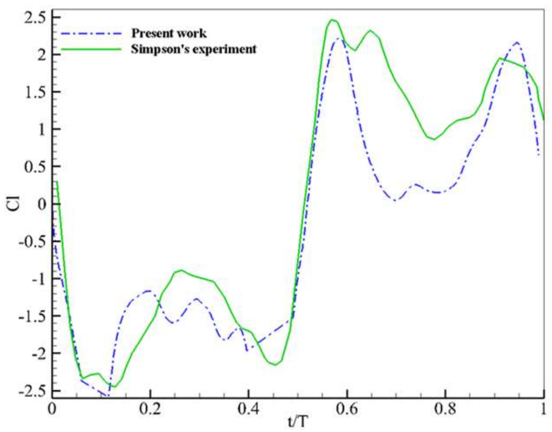

Figure 10. Cl validation with experimental work.

Table 6. Comparative analysis of Cl_{RMS} with experiment.

	Cl_{RMS}
Present work	1.65
Simpson J. [6]	1.45

This study obtained higher RMS lift coefficient of 1.654 compared to Simpson's results of 1.45.

● Results and discussion

- Large eddy simulation (LES) model is employed to provide detailed and accurate predictions of turbulent flows under NACA 0012 heaving-pitch motions.
- After grid independence test, Grid 3 was selected ensuring a balance between accuracy and computational efficiency.
- The AC DBD plasma actuator improves the aerodynamic performance of the airfoil under heave-pitch motions.
- The linear mass-spring system provides 2-DOF (heave-pitch motions) control of the airfoil and is expressed by dynamicMeshDict in OpenFOAM.

● Flow field and turbulence model under different AOAs

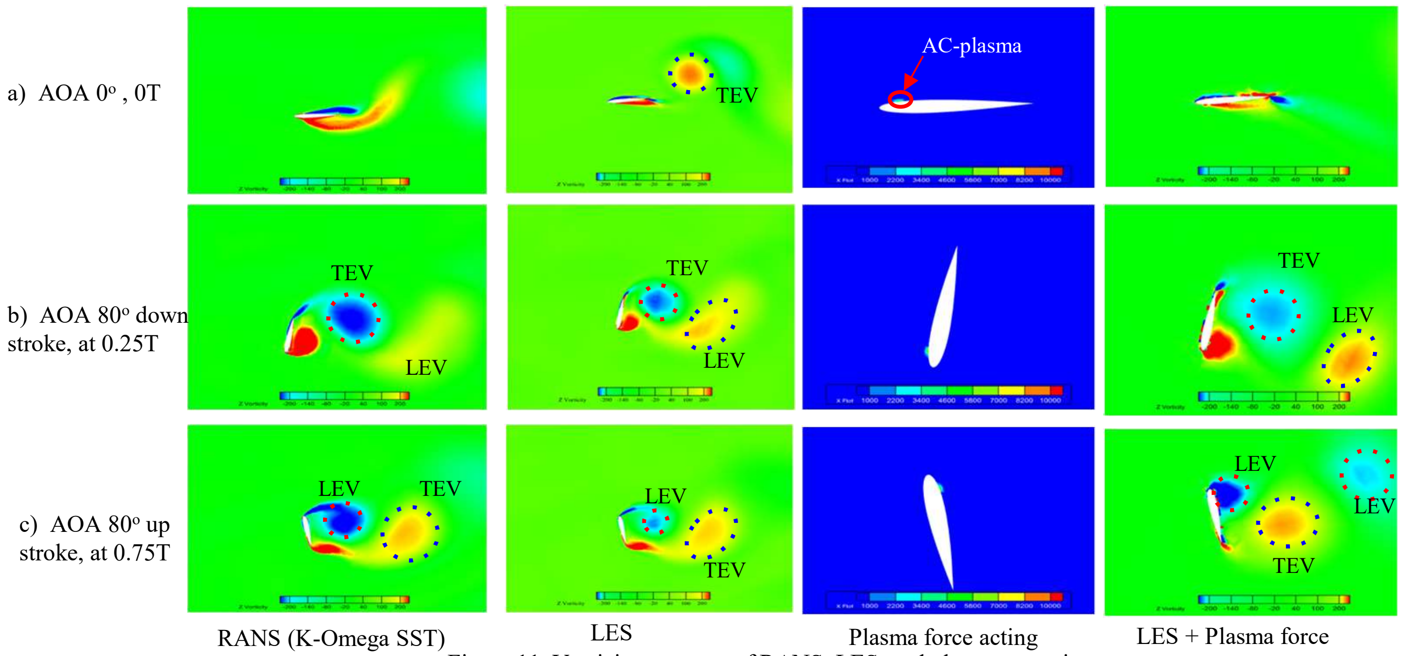

Figure 11. Vorticity contours of RANS, LES, and plasma actuations.

● A comparison of LES, RANS, and plasma actuation

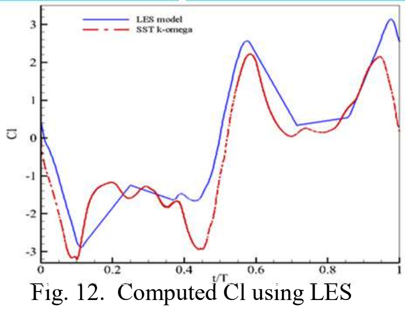

Fig. 12. Computed Cl using LES and SST k-omega.

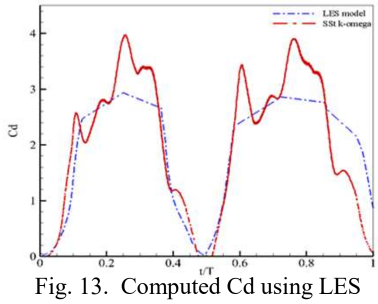

Fig. 13. Computed Cd using LES and SST k-omega.

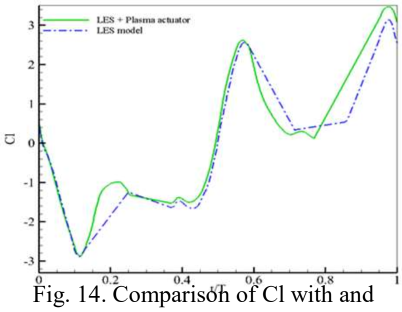

Fig. 14. Comparison of Cl with and without plasma actuation.

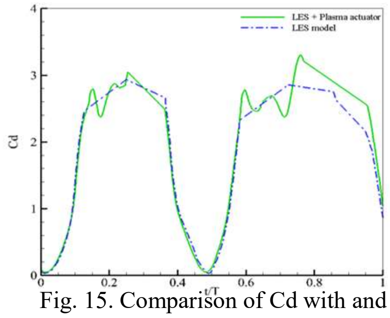

Fig. 15. Comparison of Cd with and without plasma actuation.

LES provides more accurate predictions of lift and drag coefficients shown in figures 12 and 13. RANS exhibits a significantly higher Cd values.

The LES case with plasma actuation increases the Cl and Cd values compared to the case without plasma actuation shown in figures 14 and 15.

Parameter	**Without plasma**	**With plasma**	**Improvement(%)**
Maximum lift coefficient	3.02	3.4	11.17 %
Average drag coefficient	1.24	1.25	0.8 %

● Conclusions and future work

- LES model captured detailed turbulent structures and was found to be better than RANS model.
- Utilized a linear mass-spring system analogy to analyze heave-pitch motions to gain insights into airfoil stability and response characteristics.
- The plasma actuator increases the maximum lift coefficient Cl_{max} by 11.17%, which shows the effect of plasma actuation on the NACA 0012 airfoil.

Future work

- Investigate the combined aerodynamic behavior of heave, pitch, and roll (3-DOF) on the NACA 0012 airfoil to understand their influence on lift, drag, and flow dynamics.
- Apply NS-plasma actuation technique to enhance the aerodynamic performance of NACA 0012 airfoil.

CPRG Computational Physics Research Group | National Taipei University of Technology 18 Jul 2024 Page 8